Vol.3 No.1 Jan 2020

Journal of Computational Mechanics, Power System and Control

Received 15 September, Revised 2 November, Accepted 27 December

Hybrid OBL-GO Algorithm to Support Damping Oscillations in Coordinated Control of UPFC and TCSC

Harish Kumar V C

Department of Electrical Electronics Engineering
NSS Polytechnic College
Pandala, Perumpulickal, India
vcharishkumar6@gmail.com

Amala Shanthi S

Department of Electrical Communication Engineering
NICHE
Kumaracoil, Thuckalay, India

Abstract: When controlling the stability of the power system, a suitable oscillation damping is a forthcoming major demand. Usually, this oscillation takes place owing to the variation established, while two systems are interlinked. Moreover, this work focuses on the oscillation resulted in the power system as the primary demand that hence acts as valid experimentation in the 68- bus system. Here, it develops a satisfactory CC with two FACTS devices like Unified power flow controller (UPFC) and Thyristor Controlled Series Capacitors (TCSC) that are associated with Power System Stabilizer (PSS). Significantly, it uses the Hybrid OBL-GOA approach to set up the CC between the FACTS devices. To the later of the experimentation, this work evaluates the performance of the proposed model with existing optimizations such as Gravitational Search Algorithm (GSA), Artificial Bee Colony (ABC), Particle Swarm Optimization (PSO), and Genetic Algorithm (GA), approach to set up the CC. Significantly, it requires a comprehensive study on the effect of loading aspects and PSS in CC. Consequently, the Hybrid Opposition Based Learning (OBL)-Grasshopper Optimization Algorithm (GOA)-CC performance controls against the stable power system with dynamic oscillations damping, subsequent to the evaluation of the proposed model over the conventional approaches.

Keywords: Oscillation Damping; FACTS; UPFC; TCSC; Optimization Algorithm

Nomenclature

Abbreviations	Descriptions
UPFC	Unified power flow controller
PSO	Particle Swarm Optimization
VSC	Voltage Source Converter
GSA	Gravitational Search Algorithm
FACTS	Flexible Ac Transmission System
OBL	Opposition-based Learning
GA	Genetic Algorithm
OPF	Optimal Power Flow
ABC	Artificial Bee Colony
AI	Artificial Intelligence
TCSCs	Thyristor Controlled Series Capacitors
APLFs	Active Power Loop Flows
PSS	Power System Stabilizers
GOA	Grasshopper Optimization Algorithm
MPC	Model Predictive Control
MMC-UPFC	Multilevel Converter based UPFC
NYPS	New York power system
CC	Coordinated Control
MGGP	Multi-Gene Genetic Programming
NETS	New England test system
D-FACTS	D-Distributed FACTS
LFO	Low-Frequency Oscillations
SGGP	Single-Gene Genetic Programming

https://doi.org/10.46253/jcmps.v3i1.a3

1. Introduction

All over the world, electricity demand is growing fast with society's urbanization. In power systems, to convene this massive obligation, electricity is incessantly increasing and appropriate progressively multifaceted. In a complex system, several kinds of the issue might happen throughout its process. Between the stability of the power system is considered the main problem [1]. Transient instability is encountered by a power system while it is dealt with a rapid and considerable probability. Also, in a power system, minimum oscillations of frequency might take place owing to several disturbances like deviations in a generation, faults and load, in transmission lines. In the power system, for large scale wind firm, the miniature stability of the signal angular has been studied [2]. These oscillations did not merely degrade the power system stability although it might lead to a mechanical loss if not detached or quite damped. Since the issue instability of the power system was a demanding problem for power system researchers and engineers. In nonlinear and complex dynamics, the power systems are greatly endowed and it able to encompass numerous operation points. At contingency, the nonlinearity turns out to be popular. In this condition, the existing controllers are irrelevant at a single operating point; they are useful [2].

UPFC is one of the potent and resourceful FACTS devices. It has several functions like line compensation of impedance, damping, and voltage regulation; phase shifting, power oscillation dynamic damping, impedance, and concurrent voltage control, and phase [5]. The existing VSC on the basis of the UPFC possesses restricted power and a rating of voltage, and a further low waveform output for the purpose of the restriction of voltage output levels.

Variable-impedance series FACTS gives effectual flow control of power; it is a vital provider to smart systems transmission that assures adequate employment of the conventional transmission network and holds further continuous power delivery. Nevertheless, in the power system, the improvement of FACTS devices, and the power electronic devices demands, has reported advantageous outcomes for improvements of voltage stability, electric network stability, and OPF [11]. Amid numerous FACTS devices in second-generation, UPFC is one of the prominent ones which is set up of shunt FACTS controllers and independent series [18]. It can balance three power system parameters such as phase angle, bus voltage, and line reactance among two buses [12]. Owing to this alteration ability, UPFC discovers its function in the enhancement of transportation of the power via the line of the transmission, improvement in the stability of the voltage, harmonic interaction and stability of the power system [13] [14]. Using the controller of the UPFC these tasks are performed that lead to the parameters of the system to differ as required. Throughout disturbances, the coordinated operation of PSS and UPFC can provide stability of the system and hold back LFO [15]. The appropriate parameter settings choice for the UPFC synchronized with PSS influences and its efficiency in LFO damping out. Numerous AI methods have been presented in various researches to discover the best parameters of the PSS synchronized with UPFC [16] [17].

The main contribution this work is oscillation damping which resulted in a 68- bus system. During the relation of two systems, the fluctuation leads to produces an oscillation. Therefore, in this examination, two FACTS devices like UPFC and TCSC are interconnected to the 68-bus system with PSS connection observed by Hybrid OBL-GOA based optimization to stimulate the adequate CC that accordingly minimizes the oscillation engendered in the system with UPFC and TCSC.

2. Literature Review

In 2018, Asim Haldera et al [1], developed a novel non-linear control model of TCSCs to investigate the stability of a transient condition in a power system. The non-linear control scheme was developed for the controller of TCSC using the Zero dynamic model technique. A WSCC type three-machine six-bus system had been dealt with for the test system whereas two numbers of TCSC controllers were located close to the largest load bus in the network. By inspecting the internal conditions stability and the extraneous conditions of the system, the dynamic stability of the system was accomplished. By the Lyapunov stability theorem, the stability of the internal state was assured and the extraneous conditions were stabilized by developing non-linear control rule, which was devised using the zero dynamic model technique.

In 2020, Shenghu Li et al [2] studied the setting of the active power range controllable for the UPFC in order to evade the APLFs. The sensitivity among the flow of the active power for the vital branch in addition to the active power setting for the UPFC was introduced, and iteratively worked out to discover the minimal settings of the power generation. By the max/ min minimal power settings, the settings of active power range controllable to shun the APLFs were resolved. The integrated design among the shunt and series converters was recently presented. Moreover, to convince the test of the rectangular method, the Floyd-Warshall method was enhanced, then to detect the vital branches and APLFs.

In 2020, Qiufan Yang et al [3], developed an MPC technique to deal with the control flow of the power is unbalanced grid states for the Standard MMC-UPFC. For MMC-UPFC, the predictive designs which correlate to the discrete-time designs were determined. The MMC series employs a cost function with constraints of voltage to restrain the liability current and create the flow controllable of the power, and consequently evade the fault spread. In addition, it creates complete exploit of the MMC capability through administrating it on the boundary of the voltage which was explained using the utmost converter output voltage.

In 2019, Md Shafiullah et al [4] developed an MGGP technique to optimize PSS parameters corresponding with UPFC to improve the stability of the power system using LFO damping. Moreover, attained outcomes for the developed MGGP technique were evaluated by means of the consequences of the existing predetermined gain design, and also with the SGGP technique. In addition, the satisfactory standard values of statistical metrics performance were obtained by evaluating the parameters of PSS-UPFC that offer the assurance in the developed MGGP technique.

In 2019, Yuanrui Sang and Mostafa Sahraei-Ardakani [5], developed a computationally competent stochastic distribution technique for Distributed-FACTS. Additionally, it examines their effect on flows of power. The minimization in renewable energy limitation and operation cost, attained by D-FACTS, was evaluated with that of existing FACTS. The outcomes were developed in an extensive assortment of cases to imitate the altering and an unsure circumstance in the prospective.

3. Dynamic System Model

Generally, the latest power system includes generators with their own the action of exciting systems, TCSC and PSS, network transmission and loads, and so on that exists on the FACTS devices. Further, a methodical design of the essential aspects is the key element that compromises the investigation that linked to the power system dynamic behavior. By a set of DAEs, such modeling is formulated that is independently illustrated as below.

Generator: According to the rules of the IEEE transmission, the designs of the sub-transient with four equal designs are exploited to describe the power system generators. Moreover, it is required to eradicate the sluggish- dynamics of the committee and allocates the mechanical torque because of the inputs constant. The subsequent formulations illustrate the differential formulation concerning the dynamic behavior i^{th} generator.

In the subsequent formulations, i^{th} generator is indicated by a superscript n, ω^B indicates the angular speed at the rotor base with unit radius/second, δ indicates the rotor angle with unit radians, S^m indicates the slip, K indicates the inertia constant in seconds, ω indicates the rotor and ω^B indicates synchronous angular velocity, in eq. (2) T^e indicates electrical torque and T^m indicates mechanical and D indicates the damping of the machine rotor. Additionally, in Eq. (3) E'^d and E'^q indicates the EMFs transient owing to flux field interconnections concerning q- and d-axis correspondingly, In Eq. (3) ψ_1^d and ψ_2^q indicates the EMFs sub- transient from q- axis and d-axis correspondingly, I^q and I^d indicates the current stator of the q and d-axis correspondingly, In eq. (3), Y'^d Y^d, Y''^d indicate the transient, synchronous, and reactance of the sub- transient lying in d- axis. In eq. (3), Y^q, Y'^q, Y''^q indicate the transient, synchronous, and reactance of the sub- transient lying in q- axis, U^q and U^d of eq. (4) indicate the voltage of the stator terminal of q- and d- axis correspondingly, E'^{dc} states the emf transient for the dummy rotor coil, R^a indicate the armature reactance, X^{al} indicates the leakage reactance of the armature, t^{dc} states the time constant of the dummy rotor coil (0.01seconds), In eq. (6) and (7), t'^{q0} and t'^{d0} states the transient time constant of the q andd- axis correspondingly. In eq. (8) and (9), t''^{d0} and t''^{q0} states the constant time for the sub- transient of the d- axis and q- axis correspondingly.

$$\frac{d\delta^i}{dt} = \omega^B(\omega^i - \omega^s) = \omega^B S^{mi} \tag{1}$$

$$2K^i \frac{dS^{mi}}{dt} = (T^{mi} - T^{ei}) - D^i S^{mi} \tag{2}$$

$$T^{ei} = E'^{di}I^{di}\frac{\left(Y''^{qi} - Y^{ali}\right)}{\left(Y'^{qi} - Y^{ali}\right)} + E'^{qi}I^{qi}\frac{\left(Y''^{di} - Y^{ali}\right)}{\left(Y'^{di} - Y^{ali}\right)} - I^{di}I^{qi}\left(Y''^{di} - Y''^{qi}\right) + \psi_1^{di}I^{qi}\frac{\left(Y'^{di} - Y''^{di}\right)}{\left(Y'^{di} - Y^{ali}\right)} - \psi_2^{qi}I^{di}\frac{\left(Y'^{qi} - Y''^{qi}\right)}{\left(Y'^{qi} - Y^{ali}\right)} \tag{3}$$

$$jI^{di} + I^{qi} = \left\{ \begin{array}{l} E'^{qi}\frac{\left(Y''^{di} - Y^{ali}\right)}{\left(Y'^{di} - Y^{ali}\right)} + \psi_1^{di}\frac{\left(Y'^{di} - Y''^{di}\right)}{\left(Y'^{di} - Y^{ali}\right)} - V^{qi} \\ + j\left[E'^{di}\frac{\left(Y''^{qi} - Y^{ali}\right)}{\left(Y'^{qi} - Y^{ali}\right)} - \psi_2^{qi}\frac{\left(Y'^{qi} - Y''^{qi}\right)}{\left(Y'^{qi} - Y^{ali}\right)} - V^{di} + E'^{dci}\right] \end{array} \right\} 1 \big/ \left(R^{ai} + jY''^{di}\right) \tag{4}$$

$$t^{dci} = \frac{dE'^{dci}}{dt} = -E'^{dci} + I^{qi}\left(Y''^{di} - Y''^{qi}\right) \tag{5}$$

$$t'^{q01} = \frac{dE'^{dci}}{dt} = E'^{di} + \left(Y^{qi} - Y'^{qi}\right)\left\{-\psi_2^{qi} - E'^{di} + \frac{\left(Y'^{qi} - Y''^{qi}\right)}{\left(Y'^{qi} - Y^{ali}\right)^2}\left(\left(Y'^{qi} - Y^{ali}\right)I^{qi}\right) - I^{qi}\right\} \tag{6}$$

$$t'^{d01} = E_f^{di} - E'^{qi} + \left\{-E'^{di} + I^{di} + \frac{\left(Y'^{di} - Y''^{di}\right)}{\left(Y'^{di} - Y^{ali}\right)^2}\left(\psi_1^{di} - \left(Y'^{di} - Y^{ali}\right)I^{di}\right)\right\}\left(Y^{di} - Y'^{di}\right) \tag{7}$$

$$t''^{d01}\frac{d\psi_1^{di}}{dt} = \left(Y'^{di} - Y^{ali}\right)I^{di} + E'^{qi} - \psi_1^{di} \tag{8}$$

$$t''^{q01}\frac{d\psi_2^{qi}}{dt} = \left(Y'^{qi} - Y^{ali}\right)I^{qi} + E'^{di} + -\psi_2^{qi} \tag{9}$$

Excitation system: By taking into consideration of two kinds of Automatic Voltage Regulators (AVR) and the excitation of the generators is decided. Moreover, the primary kinds are owned by the IEEE benchmark DC exciter (DC4B) and the second kind is owned by the Standard Static Exciter (ST1A). As stated in eq. (10) to eq. (14) and eq. (15), the ST1A and DC4B operation are stated in a differential formulation. In eq. (10) to eq. (14), E_f^d refers the field excitation voltage with $E_f^{d\,min} \le E_f^d \le E_f^{d\,max}$, U^a indicates the regulator emf with $E_f^{d\,min} \le V^a \le E_f^{d\,max}$, G^f state the gain of the stabilizer and G^e state the gain of the exciter, t^r states the input filter time constant, t^e states the time constant of the exciter, t^f states the time constant of the stabilizer, t^a states the time constant of the regulator, A_{ex} and B_{ex} represents the saturation constants, U^f represents the emf of stabilizer, U^r represents the input filter emf, U^{PID} represents the EMF of PID controller with $E_f^{d\,min} \big/ G^a \le U^{PID} \le E_f^{d\,max} \big/ G^a$, U^{ss} indicate the output reference voltage of PID, and U^{ref} indicate the reference voltage, and C^p, C^i, C^d, T^d represents the PID- controller parameters. Conversely, G^A states the static regulator gain in Eq. (15).

$$t^e\frac{dE_f^d}{dt} = U^a - \left(G^eE_f^d + E_f^dA_{ex}e^{B_{ex}E_f^d}\right) \tag{10}$$

$$t^r\frac{dU^r}{dt} = -U^r + U^t \tag{11}$$

$$t^f\frac{dU^f}{dt} = E_f^d - U^f \tag{12}$$

$$t^a\frac{dU^a}{dt} = G^aU^{PID} - U^a \tag{13}$$

$$U^{PID} = \left(-U^r + U^{ref} + U^{ss} - \frac{G^f}{t^f}\left[E_f^d - U^f\right]\right)\left[C^p + \frac{C^i}{s} + \frac{sC^d}{sT^d + 1}\right] \tag{14}$$

$$E_f^d = G^A\left(U^{ref} + U^{ss} - U^r\right) \tag{15}$$

Stabilizers in power system: To damp the power system local modes, PSS is exploited as a preservative system despite the excitation control for the generators. For that reason, the rotor speed, generated real power, the terminal voltage of the generator, and reactive power are represented as the PSS feedback signal. Actually, the signal that is selected must possess tremendous controllability and observability. Eq. (16) indicates the PSS dynamic equation, while S^m is exploited as the feedback signal, whereas G^{pss} refers to the gain of PSS, t^{i1} and t^{i2} states the i^{th} phase lag and lead time constants correspondingly and t^{w} states the washout time constants.

$$U^{ss} = G^{pss} \frac{st^{w}}{\left(1+st^{w}\right)} \frac{\left(1+st^{11}\right)\left(1+st^{21}\right)\left(1+st^{31}\right)}{\left(1+st^{12}\right)\left(1+st^{22}\right)\left(1+st^{32}\right)} S^{m} \tag{16}$$

Interface loads with and network equations: Generally, the basic reference encompass of the network must be chosen up to define the algebraic network equation. Additionally, using a rotor phase angle, it is taken to rotate the voltage and current, and the ensuing formulations are performed in eq. (17) and eq. (18). In addition, to connect the generator entry, the generator is indicated as a source of the current injection with the network entry that is stated by $I^{gi} = \left(I^{Qi} + jI^{Di}\right) + X^{gi} + U^{gi}$ whereas $Y^{gi} = 1 / \left(R^{ai} + jY''^{di}\right)$. The model $d(X^{G1}, X^{G1}, \ldots, X^{GN})$ indicates the entry matrix of the generator X^{G} whereas *d* stands the diagonal, N state the total count of bus nodes, as well as $X^{Gj} = X^{gi}$ is a further pattern if i^{th} generator is connected to the j^{th} node. Let the injection of the current merely on the generator buses, the ensuing injection of the current column vector at j^{th} element is $I^{j} = I^{gi}$, if i^{th} generator is connected to the j^{th} node and or else $I^{j} = 0$, for $j = 1 \text{ to } N$.

$$I^{Qi} + jI^{Di} = e^{j\delta i}\left(I^{qi} + jI^{di}\right) \tag{17}$$

$$U^{gi} = U^{Qi} + jU^{Di} = e^{j\delta i}\left(U^{qi} + jU^{di}\right) \tag{18}$$

$$V = Z^{A} I \tag{19}$$

$$Z^{A} = \left(X^{A}\right)^{-1} \tag{20}$$

In addition, the amplified entry matrix is in the form $X^{A} = X^{L} + X^{G} + X^{N}$ and U in eq. (20) indicates the column vector of the bus voltages.

4. Dynamic System Model Hybrid OBL-GOA based Coordinated Control

4.1. System Process

Fig 1 shows the proposed Hybrid OBL-GOA based CC method as an iterative procedure. Moreover, from the inter-area system design, the system response is composed that attains the line data and bus data of diverse power systems. Moreover, to decide the objective function, the extracted system response is exploited which effectuates or controls the CC using the Hybrid OBL-GOA approach. Moreover, the system possesses to use control of coordinated among the UPFC and TCSC devices. Here, the solution vector is updated by Hybrid OBL-GOA episodically on the basis of the objective function quality. Furthermore, the ensuing response of the system is considered for damping of the oscillation by the organized FACTS devices. Moreover, this procedure is reiterated numerous stages, till the system stable is obtained and consequently, it has the ability to show implied feedback on the basis of the CC using Hybrid OBL-GOA approach.

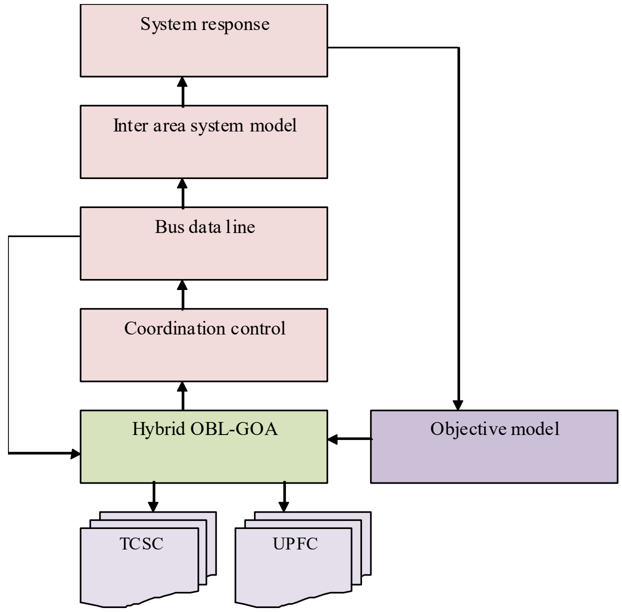

Fig. 1. *Schematic illustration of the proposed based coordination control*

4.2. Objective Model for Control

In this experimentation, the main objective is to minimize the T_s which represents the settling time, when controlling a system stable. Mainly, T_s represents the time needed for the operation to determine within a specific percentage for the amplitude input. Let consider the second-order system,

$$L\frac{d^2x(t)}{dt^2} = f(t) - A\frac{dx(t)}{dt} - Jx(t) \tag{21}$$

$$L\left(s^2X(s) - sx(0) - x'(0)\right) = F(s) - A\left(sX(s) - x(0)\right) - JX(s) \tag{22}$$

Replacement $x'(0) = 0$ in Eq. (22)

$$Ls^2X(s) + AsX(s) + JX(s) = Lsx_0 + Ax_0 + F(s) \tag{23}$$

$$X(s) = \frac{(Ls + A)x_0}{Ls^2 + As + J} + \frac{F(s)}{Ls^2 + As + J} \tag{24}$$

Let the initial term only and eq. (26) indicates the second-order system,

$$X(s) = \frac{\left(s + A/L\right)x_0}{s^2 + \left(A/L\right)s + J/L} = \frac{\left(s + 2\zeta\omega_n\right)x_0}{s^2 + 2\zeta\omega_n s + \omega_n^{\,2}} \tag{25}$$

$$e^{-\zeta\omega_n T_s} < 0.02 \Rightarrow \zeta\omega_n T_s = 4 \tag{26}$$

$$T_s = \frac{4}{\zeta\omega_n} = 4\tau \tag{27}$$

In Eq. (27), ζ shows the ratio of the dimensionless damping as $\zeta = \frac{A}{2\sqrt{JL}}$ and ω_n shows the natural frequency as $\omega_n = \sqrt{\frac{J}{L}}$.

5. Optimal Compensation and Location

5.1. Procedure of GOA

In [8], proposed the GOA swarm approach that imitates the grasshopper's behavior is illustrated. These grasshoppers are a pest class which affects agriculture and production of the crop, and their development comprises of three stages such as adulthood, nymph, and egg, [9]. In the nymph stage, the most important features for the movement of grasshopper in rolling cylinders which comprises moving and jumping (by means of slow movements and least steps), and they consume vegetation established in their route. In a swarm, Grasshoppers migrates in a long-distance (by means of extended-range and sudden movements) in the adulthood stage. These behaviors are mathematically devised by taking into consideration of the location of the grasshopper (y_i) as below [8] [9]:

$$y_i = SC_i + GF_i + WA_i \tag{28}$$

In eq. (28), SC_i represents interaction in socially in the i^{th} grasshopper and it is stated in eq. (29).

$$SC_i = \sum_{j=1, i\neq j}^{N} s(d_{ij})\hat{d}_{ij}, \quad d_{ij} = |y_i - y_j| \tag{29}$$

In eq. (29), d_{ij} states the distance among i^{th} and j^{th} Grasshoppers; when s states the power of social forces model which is stated in eq. (30).

$$s(z) = f\ e^{\frac{-z}{l}} - e^{-z} \tag{30}$$

In eq. (30), l and f indicate the length scale attraction and the intensity of the attraction. In Eq. (28), GF_i and WA_i indicate the wind advection and force of the gravity for the i^{th} grasshopper, correspondingly and it is stated in eq. (31).

$$GF_i = -g\hat{e}_g,\ WA_i = u\hat{e}_w \tag{31}$$

In eq. (31), u indicate a constant drift and g indicate the gravitational constant; when $\hat{e}_w$ and $\hat{e}_g$ indicate the vector unity in the direction of the wind and the earth center, correspondingly. Nevertheless, Eq. (28) should not be used directly to discover the optimization solution issue, consequently, in [8] reformulated it is stated in eq. (32).

$$y_i = c\left(\sum_{j=1, i\neq j}^{N} c\frac{u-l}{2} s(|y_j - y_i|)\frac{y_j - y_i}{d_{ij}}\right) + \hat{T}_d \tag{32}$$

In eq. (32), l and u indicate the search spaces lower and upper bound, correspondingly;

T_d indicates the value of the best solution established so far; and as in eq. (30) s is explained. Nevertheless, in eq. (32) gravity is not taken, and the direction of the wind is forever represented toward $\hat{T}_d$. Moreover c describes a minimizing shrink coefficient the attraction, and zone, and repulsion zone and it is stated below:

$$c = c_{max} - t\frac{c_{max} - c_{min}}{t_{max}} \tag{33}$$

In eq. (33), t indicate the iteration for current values, c_{min} and c_{max} indicate the minimum c value which is equivalent to 0.00001 and a maximum c value which is equivalent to 1, correspondingly; and t_{max} indicate the utmost number of iterations. Moreover, the GOA initiates by producing an arbitrary population Y of size N. For each solution y_i, $i = 1, \ldots\ldots, N$, to compute the fitness model subsequent step is used and the optimal solution, $\hat{T}_d$, indicate subsequently chosen consistent with the optimal fitness model. Afterward, for every y_i, the subsequent 2 steps are done such as a) among the solutions the distance normalization in Y is [1, 4]; and b) update the current solution y_i. The current iteration is updated using the subsequent step is exploited and do again the preceding steps until the terminating circumstances are attained.

5.2. Procedure of OBL

The OBL scheme is exploited for the current solution in order to describe the conflicting solution, and it subsequently exploits the value of the fitness function (f) to decide if the conflict is superior to the current solution. The fundamental explanation of the OBL is described in [10], using presumptuous the value of conflicting $\bar{y}$ for the value of the real $y \in [u, l]$ that is computed by using eq. (34).

$$\bar{y} = u + l - y \tag{34}$$

This description can be widespread to n–dimensions exploiting eq. (35).

$$\bar{y}_i = u_i + l_i - y_i \quad i = 1, 2, \ldots\ldots, N \tag{35}$$

In eq. (35), from the real vector $y \in R^n$, $\bar{y} \in R^n$ indicates the conflicting vector. Additionally, by the optimization procedure, the 2 solutions (y and $\bar{y}$) are evaluated, and the solutions optimal is saved, when erstwhile is eradicated using fitness model evaluation. For instance, if $f(y) \leq f(\bar{y})$ (for reduction), subsequently y is stored; or else, $\bar{y}$ is saved.

5.3 Proposed Hybrid OBL-GOA

This paper demonstrates the hybrid technique design in order to enhance the GOA performance approach. In this circumstance, GOA is enhanced using integrating its novel model by means of the OBL scheme. Moreover, to intensely discover the domain of the search to develop the capability and fast attains the value of the best. Fig 2 shows the flow chart of the proposed Hybrid OBL-GOA method.

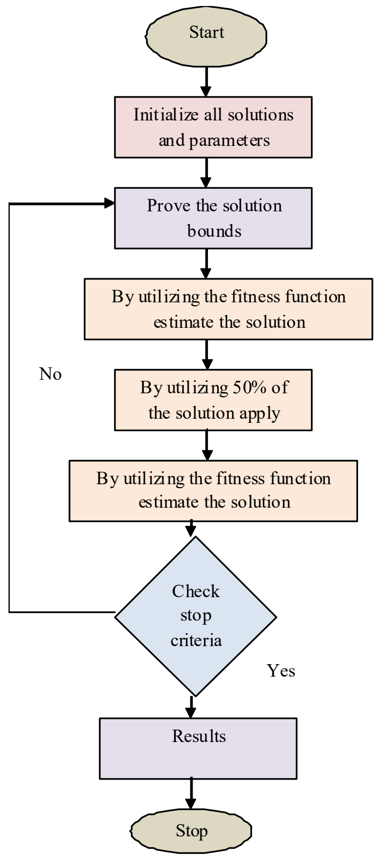

Fig. 2. *Flow chart of the proposed hybrid OBL-GOA algorithm*

The OBL scheme is used subsequent to concluding the GOA's exploration stage to uphold 50% of the domain space which has been computed using the GOA. This step permits the original domain space to attain the best value rapidly and mend the out-of-range values. Generally, the proposed Hybrid OBL-GOA comprises two phases such as the initial stage and the updating stage.

The explanation of these phases is proposed as stated as follows.

In the initial phase, the Hybrid OBL-GOA technique starts by deciding the preliminary values of the parameter for GOA; subsequently, in dimension, $\dim$ the GOA arbitrarily produces a N population size. For each solution, the OBL is exploited in the population to compute the conflicting solution. In addition, each solution in Y as well as $\overline{Y}$, the fitness model is computed. In the initial phase, the optimal N solutions are chosen by the concluding step from the two union populations (Y as well as $\overline{Y}$).

In updating phase, in accordance with eq. (32), each solution is updated and estimated by exploiting the fitness model. Then, the optimal solution and fitness value are stored. Simultaneously, from the GOA, the OBL method obtains the updated solutions and chooses a number of 50% by using this population of conflicting in order to compute this element. Here, in this element the solutions that stand for optimal 50% in accordance with the fitness models.

Then, by using the fitness model, the consequence is revaluated; if the value of the fitness is superior to the current value, in the subsequent iteration, the Hybrid OBL-GOA is exploited to update the value of this population.

This method is reiterated until the termination circumstance is met (here, Hybrid OBL-GOA exploits the utmost number of iterations as a halt condition).

6. Results and Discussions

6.1. Simulation Setup

The perception related to the damping of the oscillation for the system was carried out in the 68- bus system. For equal interconnected NYPS and NETS, the 68- bus system was minimized. For that reason, this model consists of 5 geographical areas. Amid such areas, a set of generators was exploited to stand for NETS and NYPS. Additionally, a suitable generator model was developed from adjacent regions to introduce power. Fundamentally, the 68- bus system rotor models were exploited to be round. However, the generator 9 comprises ST1A and complete system generators comprise DC4B. Especially, PSS was linked to the generators one to twelve. With the system, the loads related were almost certainly constant impedance form.

6.2. Performance Anlaysis

Table 1 summarizes the various G15 constraints, with an evaluation of developed and existing techniques. Moreover, proposed is compared with the conventional algorithms with numerous constraints. Yet, all the constraints attain the least values for the proposed algorithm that is better than the existing algorithms.

Table 2 shows the evaluation related to the loading effects of the developed technique in the 68- bus system via the purpose of several constraints. That constraints comprise peak, settling time, undershoot, rise time, maximum settling, minimum settling, overshoot, and peak time. Moreover, at no load circumstance, these constraints are decided beside 20%, 60%, and 80% 40%, and100% of load circumstance. Concerning, undershoot; the least value is attained at 80% for load circumstance while the least overshoot happens at 100% of load circumstance.

Table 1. *Calculation of G15 using the proposed and existing techniques*

Techniques	Overshoot	Maximum settling	Peak	Rise time	Settling time	Minimum settling	Undershoot
GSO-CC	71245.6	1.02 e^{-05}	1.11 e^{-05}	12.62348	1564.7	-1.2e^{-05}	72605.9
ABC-CC	229334	8.30 e^{-06}	9.20 e^{-06}	0.563478	1619.59	-1.2 e^{-05}	243264
GA-CC	45326.7	9.12 e^{-06}	9.10 e^{-06}	101.4177	1523.35	-9.8 e^{-06}	412459
PSO-CC	55912.5	1.00 e^{-05}	1.10 e^{-05}	102.437	1547.82	-9.5 e^{-06}	56124.4
FF-CC	11755.8	1.15 e^{-05}	1.11 e^{-05}	1.125826	1513.48	-1.1 e^{-05}	124155

Table 2. *Comparison Analysis of Loading Analysis For The Developed Approach*

Load condition	Overshoot	Maximum settling	Peak	Rise time	Settling time	Minimum settling	Undershoot	Peak time
no load	13955.59	8.94 e^{-06}	8.94 e^{-06}	4.907796	1911.548	-8.9 e^{-06}	13971.11	4.907796
20	71585.57	1.12 e^{-05}	1.12 e^{-05}	13.62748	1684.7	-1.1 e^{-05}	73205.86	13.62748
40	55960.46	1.12 e^{-05}	1.12 e^{-05}	112.497	1687.818	-1.1 e^{-05}	57224.35	112.497
60	45382.67	9.48 e^{-06}	9.82 e^{-06}	111.4077	1733.35	-9.8 e^{-06}	43869.4	111.4077
80	229342.6	9.3 e^{-06}	9.5 e^{-06}	0.575777	1729.594	-9.5 e^{-06}	234363.5	0.575777
100	117267.8	1.15 e^{-05}	1.15 e^{-05}	1.171826	1683.481	-1.1 e^{-05}	115055.1	1.171826

7. Conclusion

By means of the improvement of complexity and for the oscillation damping range, interconnected power systems possesses occurred as the contentious interruption over the experienced stability of the system. This work has suggested experimentation of the 68- bus system by concentrating on the aforesaid concern. Moreover, the experimentation was performed with the association of two FACTS devices comprise UPFC and TCSC in a 68-bus system that possesses further established using Hybrid OBL-GOA-based optimization to provide a valued CC. This includes, sequentially, oscillation damped resulted in the power system. Furthermore, the Hybrid OBL-GOA performance-based CC was examined with conventional techniques like GSO, FF, ABC, and GA with CC and further without coordination with the system among UPFC and TCSC. Additionally, this work possesses strengthened relations without and with the connection of PSS. Furthermore, this work has suggested an explanation concerning the effects of loading and PSS effects. Eventually, it has confirmed the better performance of Hybrid OBL-GOA based CC in damping of the oscillation for the system while comparing with the existing methods.

Compliance with Ethical Standards

Conflicts of interest: Authors declared that they have no conflict of interest.

Human participants: The conducted research follows the ethical standards and the authors ensured that they have not conducted any studies with human participants or animals.

References

[1] Asim Halder, Nitai Pal, Debasish Mondal,"Transient Stability Analysis of a Multimachine Power System with TCSC Controller – A Zero Dynamic Design Approach", International Journal of Electrical Power & Energy Systems, Volume 97, April 2018, Pages 51-71.
[2] Shenghu Li, Ting Wang, Hao Zhang, Lei Wang, Jing Xue,"Sensitivity-based coordination to controllable ranges of UPFCs to avoid active power loop flows", International Journal of Electrical Power & Energy Systems, Volume 114, January 2020.
[3] Qiufan Yang, Ting Ding, Hengxin He, Xia Chen, Shu Chen,"Model predictive control of MMC-UPFC under unbalanced grid conditions", International Journal of Electrical Power & Energy Systems, Volume 117, May 2020.
[4] Md Shafiullah, Md Juel Rana, Mohammad Shoaib Shahriar, Md Hasan Zahir,"Low-frequency oscillation damping in the electric network through the optimal design of UPFC coordinated PSS employing MGGP", Measurement, Volume 138, May 2019, Pages 118-131.
[5] Yuanrui Sang, Mostafa Sahraei-Ardakani, "Effective power flow control via distributed FACTS considering future uncertainties", Electric Power Systems Research, Volume 168, March 2019, Pages 127-136.
[6] B. K. Kumar, S. N. Singh and S. C. Srivastava, "Placement of FACTS controllers using modal controllability indices to damp out power system oscillations," in IET Generation, Transmission & Distribution, vol. 1, no. 2, pp. 209-217, March 2007.
[7] Y. Y. Hsu and T. S. Luor, "Damping of power system oscillations using adaptive thyristor-controlled series compensators tuned by artificial neural networks," in IEE Proceedings - Generation, Transmission and Distribution, vol. 146, no. 2, pp. 137-142, Mar 1999.
[8] Saremi, S., Mirjalili, S., & Lewis, A, “Grasshopper optimisation algorithm: Theory and application”, Advances in Engineering Software, 105 , 30–47, 2017.
[9] Rogers, S.M., Matheson, T., Despland, E., Dodgson, T., Burrows, M., & Simpson, S. J,” Mechanosensory-induced behavioural gregarization in the desert locust schistocerca gregaria”, Journal of Experimental Biology, 206 , 3991–4002, 2003.
[10] Tizhoosh, H. R, “Opposition-based learning: a new scheme for machine intelligence. In Computational intelligence for modelling, control and automation”, international conference on intelligent agents, web technologies and internet commerce, international conference on Volume 1, pp. 695–701, IEEE 2005.
[11] R. Majumder, B. C. Pal, C. Dufour and P. Korba, "Design and real-time implementation of robust FACTS controller for damping inter-area oscillation," IEEE Transactions on Power Systems, Volume 21, Issue. 2, page number. 809-816, May 2006.
[12] H. Nguyen-Duc, L. A. Dessaint, A. F. Okou and I. Kamwa, "A Power Oscillation Damping Control Scheme Based on Bang-Bang Modulation of FACTS Signals," in IEEE Transactions on Power Systems, Volume. 25, Issue. 4, page number. 1918-1927, November, 2010.
[13] M.F. Castoldia, D.S. Sanchesa, M.R. Mansourb, N.G. Bretasb and R.A. Ramosb, "A hybrid algorithm to tune power oscillation dampers for FACTS devices in power systems", Control Engineering Practice, Volume. 24, page number..25–32, March 2014.
[14] A. Chakrabortty, "Wide-Area Damping Control of Power Systems Using Dynamic Clustering and TCSC-Based Redesigns," in IEEE Transactions on Smart Grid, Volume 3, Issue. 3, page number. 1503-1514, Sept. 2012.
[15] Mohsen Bakhshi, Mohammad Hosein Holakooie and Abbas Rabiee, "Fuzzy based damping controller for TCSC using local measurements to enhance transient stability of power systems", Electrical Power and Energy Systems, Volume. 85, page number.12–21, 2017.
[16] Kazem Zare, Mehrdad Tarafdar Hagh and Javad Morsali, "Effective oscillation damping of an interconnected multi-source power system with automatic generation control and TCSC", Electrical Power and Energy Systems, Volume.65, page number.220–230, 2015.
[17] M. Zarghami, M. L. Crow, J. Sarangapani, Y. Liu and S. Atcitty, "A Novel Approach to Interarea Oscillation Damping by Unified Power Flow Controllers Utilizing Ultracapacitors," in IEEE Transactions on Power Systems, Volume. 25, Issue. 1, page number. 404-412, Feb. 2010.
[18] Naresh Kumar Yadav,"Optimal ATC Enhancement Model: Analysis of the Effect of Thyristor-Controlled Series Compensation",Journal of Computational Mechanics, Power System and Control (JCMPS)Volume 2, Issue 1, January 2019.